Title
Kif3a interacts with Dynactin subunit p150Glued to organize centriole subdistal appendages

Journal
The EMBO Journal, 32(4)

ISSN
0261-4189

Authors
Kodani, Andrew
Sirerol-Piquer, Maria Salomé
Seol, Allen
et al.

Publication Date
2013-02-20

DOI
10.1038/emboj.2013.3

Peer reviewed

The EMBO Journal (2013) 32, 597–607
www.embojournal.org

SOURCE DATA | TRANSPARENT PROCESS | THE EMBO JOURNAL

Kif3a interacts with Dynactin subunit p150^{Glued} to organize centriole subdistal appendages

Andrew Kodani[1], Maria Salomé Sirerol-Piquer[2], Allen Seol[1], Jose Manuel Garcia-Verdugo[2] and Jeremy F Reiter[1,*]

[1]Department of Biochemistry and Biophysics, Cardiovascular Research Institute, University of California, San Francisco, CA, USA and [2]Department of Cellular Morphology, University of Valencia, Unidad Mixta CIPF-UVEG, CIBERNED, Valencia, Spain

Formation of cilia, microtubule-based structures that function in propulsion and sensation, requires Kif3a, a subunit of Kinesin II essential for intraflagellar transport (IFT). We have found that, Kif3a is also required to organize centrioles. In the absence of Kif3a, the subdistal appendages of centrioles are disorganized and lack p150^{Glued} and Ninein. Consequently, microtubule anchoring, centriole cohesion and basal foot formation are abrogated by loss of Kif3a. Kif3a localizes to the mother centriole and interacts with the Dynactin subunit p150^{Glued}. Depletion of p150^{Glued} phenocopies the effects of loss of Kif3a, indicating that Kif3a recruitment of p150^{Glued} is critical for subdistal appendage formation. The transport functions of Kif3a are dispensable for subdistal appendage organization as mutant forms of Kif3a lacking motor activity or the motor domain can restore p150^{Glued} localization. Comparison to cells lacking Ift88 reveals that the centriolar functions of Kif3a are independent of IFT. Thus, in addition to its ciliogenic roles, Kif3a recruits p150^{Glued} to the subdistal appendages of mother centrioles, critical for centrosomes to function as microtubule-organizing centres.

The EMBO Journal (2013) **32,** 597–607. doi:10.1038/emboj.2013.3; Published online 5 February 2013
Subject Categories: cell & tissue architecture
Keywords: centriole cohesion; centrosome; Kif3a; p150^{Glued}; subdistal appendage

Introduction

The centrosome is the major microtubule-organizing centre of most eukaryotic cells, and contains mother and daughter centrioles (Bobinnec *et al*, 1998). The mother centriole is distinguished from the daughter by accessory structures called the subdistal and distal appendages (Paintrand *et al*, 1992).

An electron dense cloud of material called the pericentriolar matrix (PCM) surrounds the centriole pair (Bornens, 2002; Takahashi *et al*, 2002). The PCM provides binding sites for the γ-tubulin ring complex that templates microtubule nucleation at the centrosome (Moritz *et al*, 2000). Subsequently, these microtubules become preferentially anchored to the subdistal appendages of mother centrioles, augmenting the ability of the centrosome to act as a microtubule-organizing centre (Mogensen *et al*, 2000; Piel *et al*, 2000; Chang *et al*, 2003; Delgehyr *et al*, 2005).

In addition to its role in anchoring microtubules, the subdistal appendage is required for ciliogenesis. The mother centriole is the foundation upon which the primary cilium is built, at which time it becomes known as the basal body (Ishikawa *et al*, 2005; Graser *et al*, 2007). Upon docking of the basal body at the cellular surface, intraflagellar transport (IFT) facilitates the transport of ciliary proteins from the cytoplasm to the cilium (Ishikawa and Marshall, 2011). The anterograde motor for IFT is Kinesin II, which delivers ciliary components to the tip where the axoneme is assembled (Rosenbaum and Witman, 2002; Pedersen *et al*, 2006). Consequently, disruption of the Kinesin II motor heterodimeric subunits Kif3a or Kif3b blocks mammalian ciliogenesis (Nonaka *et al*, 1998; Marszalek *et al*, 1999; Takeda *et al*, 1999). Kif3a participates in cellular processes apart from IFT, such as immune synapse formation, but its precise role in non-ciliary processes has been unclear (Sfakianos *et al*, 2007; Corbit *et al*, 2008; Finetti *et al*, 2009).

During ciliogenesis, the subdistal appendage of the basal body forms a morphologically distinct structure, the basal foot, upon which cytoplasmic microtubules are anchored (Anderson, 1972). Basal feet project orthogonally from the basal body and, when associated with non-motile cilia, are randomly orientated (Boisvieux-Ulrich and Sandoz, 1991). In contrast, basal feet of motile cilia are oriented in the direction of fluid flow and align the ciliary beat in the direction of the pulling force (Holley and Afzelius, 1986; Mitchell *et al*, 2007; Kunimoto *et al*, 2012). Consequently, ciliary basal feet are essential for planarly polarizing the ciliary stroke direction, defects in which can cause primary ciliary dyskinesia (Rayner *et al*, 1996; Mitchell *et al*, 2009; Mirzadeh *et al*, 2010; Kunimoto *et al*, 2012).

We have found that Kif3a specifically associates with the mother centriole and organizes subdistal appendages. Kif3a interacts with the Dynactin component p150^{Glued}, which facilitates bidirectional transport along microtubules and, in the absence of Kif3a, p150^{Glued} fails to localize to the subdistal appendage, disrupting microtubule anchoring and basal foot formation. These findings indicate that Kif3a is not only required for IFT within cilia, but also for centriole organization and function.

Results

Kif3a associates specifically with the mother centriole

We examined the subcellular localization of Kif3a in mouse embryonic fibroblasts (MEFs) with an antibody against Kif3a. Immunoblotting and immunofluorescence showed a loss of Kif3a in *Kif3a*$^{-/-}$ lysate and *Kif3a*$^{-/-}$ cells, confirming

*Corresponding author. JF Reiter, Department of Cardiovascular Research Building Room 384, 555 Mission Bay Boulevard South, PO Box 589001 San Francisco, CA 94158-9001, USA. Tel.: +1 415 502 8528; Fax: +1 415 476 0526; E-mail: jeremy.reiter@ucsf.edu

Received: 19 November 2012; accepted: 4 December 2012; published online: 5 February 2013

antibody specificity (Figure 1A and B). The antibody recognized a prominent focus at centrosomes of wild-type (WT) cells, as previously reported (Haraguchi *et al*, 2006). In G1 cells, Kif3a was present at one of the paired centrioles containing the centriolar distal lumen protein, Centrin (Figure 1B). Localization of Kif3a to a single centriole was maintained during G2 and mitosis (Figure 1C).

Deconvolution microscopy revealed that at the mother centriole, Kif3a localizes to a single focus (Figure 1D). This focus of Kif3a is at the same point along the proximal–distal axis of the centriole as the ring of subdistal appendages marked by Ninein and p150^{Glued}, two subdistal appendage components (Figure 1D). The localization of Kif3a is similar to ODF2, another mother centriolar protein that localizes to a single centriolar focus close to the subdistal appendages (Nakagawa *et al*, 2001; Kunimoto *et al*, 2012). Kif3a did not colocalize with the proximal centriolar component Sas6 or the daughter centriolar protein Centrobin, confirming that it is predominantly near the distal end of the mother centriole (Figure 1D).

Similar to MEFs, Kif3a localized to a domain close to the subdistal appendages of mother centrioles in HeLa and U2OS cells, non-ciliated human cells, revealed by comparing its distribution with p150^{Glued} and another subdistal appendage component, Cep170 (Guarguaglini *et al*, 2005; Supplementary Figure 1a). To further confirm that Kif3a is a centrosomal component, we isolated centrosomes from Jurkat cells and found that Kif3a co-fractionated with γ-tubulin and CP110 (Supplementary Figure 1b). Thus, Kif3a is a centrosomal component that localizes to a focus close to the subdistal appendages of mother centrioles throughout the cell cycle.

Kif3a is required for centriole cohesion and organization

Given its localization at the mother centriole, we explored how Kif3a participates in centrosome organization. In mammalian cells, the mother and daughter centriole remain tightly associated until late G1, when centriole cohesion is broken (Wong and Stearns, 2003). Immunofluorescence analysis of the centriolar components Centrin3 and polyglutamylated tubulin revealed that, without Kif3a, centriole cohesion is broken prematurely during G1 (Figure 2A). Greater than 80% of *Kif3a* mutant cells displayed separated centrioles in G1, as compared with <15% of WT and conditional *Kif3a* cells (Figure 2B). We also observed premature centriole separation in MEFs derived from embryonic day 12.5 *Kif3a*$^{flox/flox}$ embryos and infected with Cre-recombinase to delete Kif3a (Corbit *et al*, 2008; Figure 2B).

As Kif3a localized to a centriolar region overlapping with the subdistal appendages, we investigated whether loss of Kif3a affects subdistal appendage organization by examining the localization of Centrin and the subdistal appendage proteins p150^{Glued}, Ninein, and Cep170 in WT and *Kif3a* mutant cells in G1 (Ou *et al*, 2002; Louie *et al*, 2004; Guarguaglini *et al*, 2005). Interestingly, p150^{Glued}, which forms a ring near the subdistal centriole of WT cells, was absent from *Kif3a*$^{-/-}$ centrioles (24% of WT fluorescence,

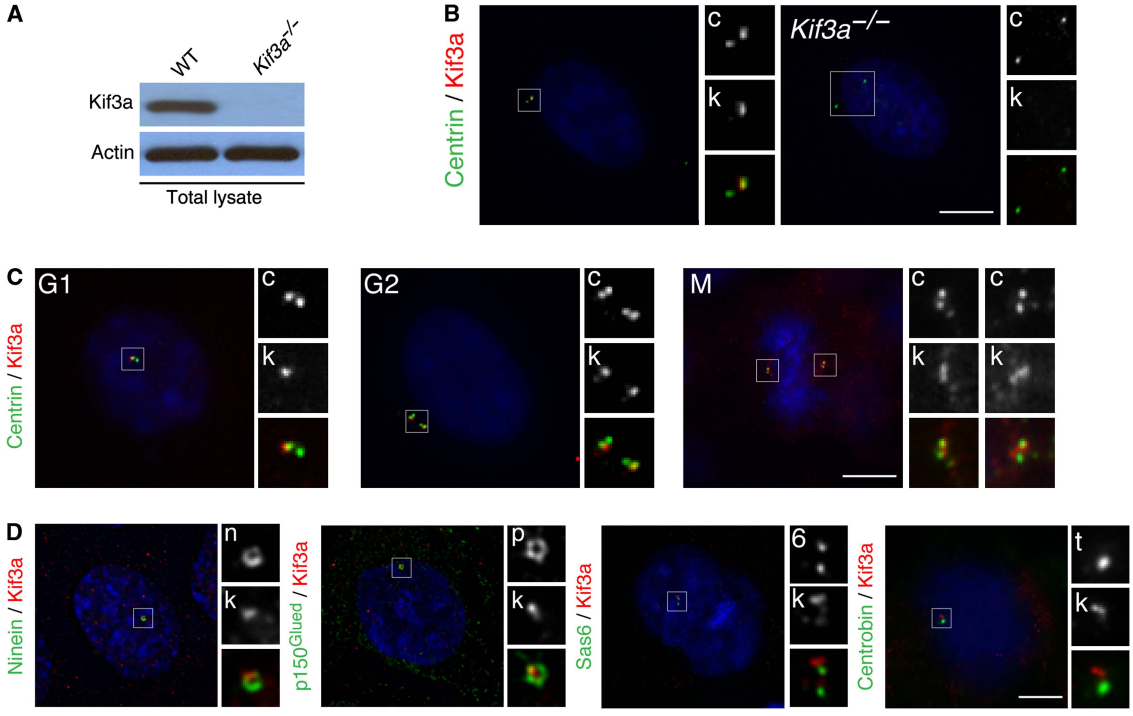

Figure 1 Kif3a localizes to the subdistal appendage of mother centrioles. (**A**) Total cell lysates of WT or *Kif3a*$^{-/-}$ MEFs were analysed by immunoblotting for Kif3a. Actin served as a loading control. 40 μg of protein lysate was loaded per lane. (**B**) Immunofluorescence microscopy analysis of WT or *Kif3a*$^{-/-}$ cells co-stained for Centrin ('c', green) and Kif3a ('k', red). The inset shows magnified images of the boxed region. (**C**) The cell-cycle-dependent localization of Kif3a was determined by examining the localization of Centrin ('c', green) and Kif3a ('k', red) in WT MEFs. Centrin and DNA organization were used to determine the cell-cycle stage. (**D**) Deconvolved immunofluorescence images of WT cells co-stained for Kif3a ('k', red), Ninein ('n', green) and p150^{Glued} ('p', green) to mark the subdistal appendage, Sas6 ('s', green) to mark the proximal ends of centrioles and Centrobin ('t', green) to mark the daughter centriole. Scale bars indicate 5 μm for images in (**B**, **C**), 3 μm for images in (**D**).

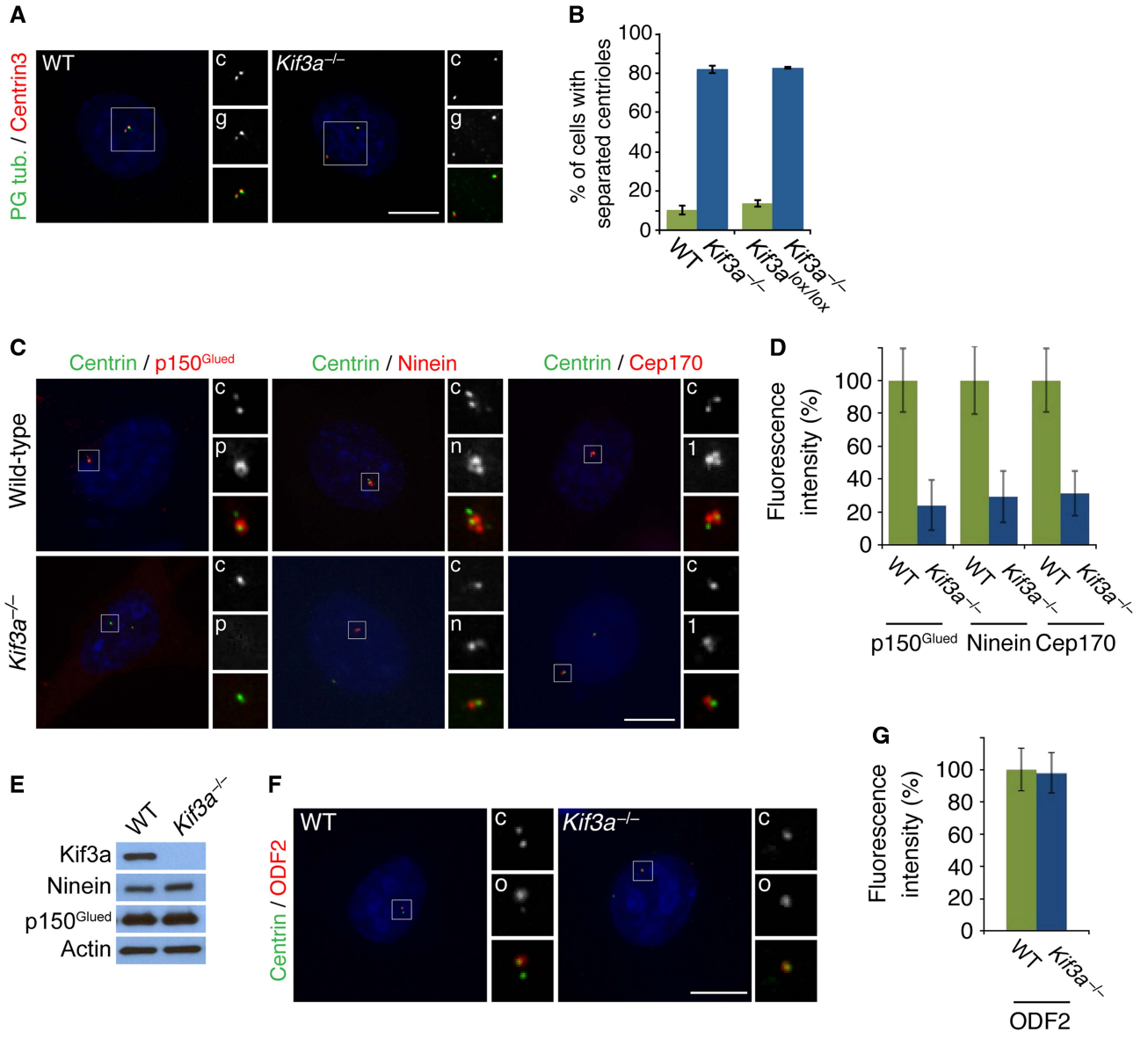

Figure 2 Kif3a is essential for centriole cohesion and subdistal appendage organization. (**A**) Immunofluorescence images of WT and *Kif3a*$^{-/-}$ cells in G1 co-stained for Centrin (red, 'c') and polyglutamylated tubulin ('g', green) to visualize centrioles. (**B**) Percentage of split centrioles in G1 for WT, *Kif3a*$^{-/-}$, *Kif3a*$^{lox/lox}$ and *Kif3a*$^{-/-}$ cells generated by Cre-mediated deletion of Kif3a. (**C**) WT and *Kif3a*$^{-/-}$ cells in G1 stained for Centrin ('c', green), p150^{Glued} ('p', red), Ninein ('n', red) and Cep170 ('1', red), to assess centriole and subdistal appendage organization. (**D**) Quantification of the mean fluorescence intensities ± s.d. of p150^{Glued}, Ninein and Cep170 in WT and *Kif3a*$^{-/-}$ cells expressed as the mean percentage ± s.d. of the fluorescence intensities in WT cells. (**E**) Total cell lysates of WT or *Kif3a*$^{-/-}$ MEFs were analysed by immunoblotting for Kif3a, Ninein and p150^{Glued}. Actin served as a loading control. 25 μg of protein lysate was loaded per lane. (**F**) Immunofluorescence images of WT and *Kif3a*$^{-/-}$ cells co-stained for Centrin ('c', green) and ODF2 ('o', red). (**G**) Quantification of the mean fluorescence intensity percentage ± s.d. of ODF2 in WT and *Kif3a*$^{-/-}$ MEFs. Scale bars indicate 5 μm for all images. For all quantifications at least 100 cells were analysed per experiment ($n = 3$), $P < 0.001$ (paired *t*-test).

Figure 2C). Similarly, Ninein was reduced on *Kif3a*$^{-/-}$ centrioles (31% of WT fluorescence, Figure 2C). On WT mother centrioles, Ninein localized to three foci one of which is proximal (Ishikawa *et al*, 2005). *Kif3a*$^{-/-}$ centrioles showed only one strong focus. Cep170, which depends on Ninein to localize to the subdistal appendage was also reduced at the mother centrioles of cells lacking Kif3a (Graser *et al*, 2007, 29% of WT fluorescence). Loss of Kif3a has no effect on the protein levels of p150^{Glued} or Ninein (Figure 2E), indicating that Kif3a participates in the organization of the subdistal appendages.

Previous studies have shown that another mother centriole component, ODF2, is required for the recruitment of Ninein to the centrosome and the organization of subdistal appendages (Nakagawa *et al*, 2001; Kunimoto *et al*, 2012). To assess whether the disruption of the subdistal appendages in *Kif3a* mutants resulted from mislocalization of ODF2, we examined ODF2 in *Kif3a*$^{-/-}$ MEFs (Figure 2F). Loss of Kif3a had no effect on the localization of ODF2 to the centrosome (Figure 2G).

To test whether the role of Kif3a in centriole cohesion and subdistal appendage formation are secondary to the

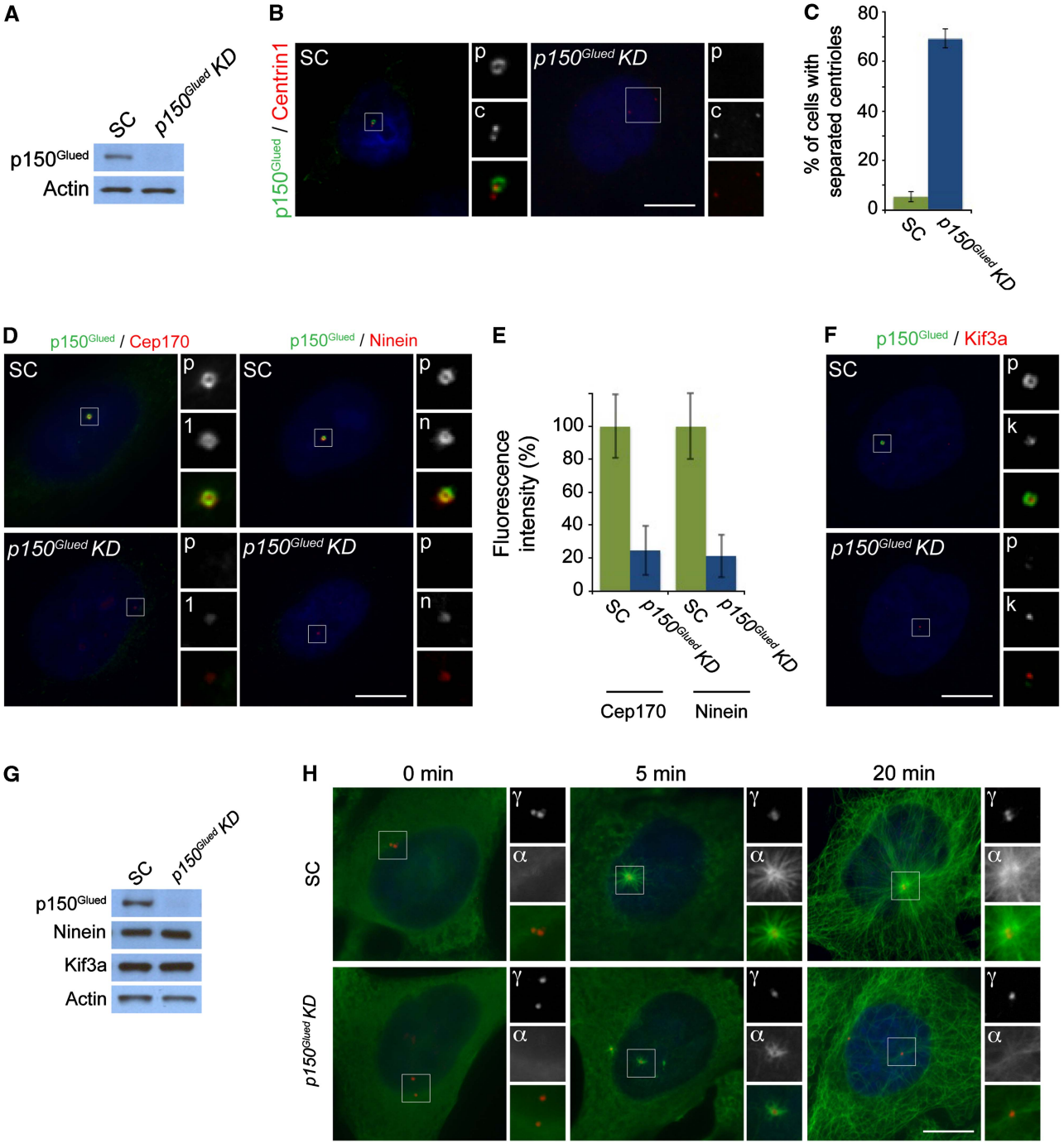

Figure 3 p150^{Glued} is required for centriole cohesion and subdistal appendage organization and function. (**A**) Total cell lysates of scramble control (SC) or *p150^{Glued}* siRNA transfected HeLa cells were analysed by immunoblotting for p150^{Glued}. Actin served as a loading control. 25 μg of protein lysate was loaded per lane. (**B**) HeLa cells in G1 transfected with SC or *p150^{Glued}* siRNA were co-stained for p150^{Glued} ('p', green) and Centrin ('c', red) to visualize centrioles. (**C**) Mean percentage ± s.d. of split centrioles in G1 for SC and p150^{Glued} transfected cells. (**D**) The depletion of p150^{Glued} ('p', green) disrupted the localization of the subdistal appendage proteins Cep170 ('1', red) and Ninein ('n', red). (**E**) Quantification of the mean fluorescence intensities ± s.d. of Cep170 and Ninein in SC and *p150^{Glued}* siRNA-treated cells. (**F**) Immunofluorescence images of SC and *p150^{Glued}* siRNA-treated HeLa cells co-stained for p150^{Glued} ('p', green) and Kif3a ('k', red). (**G**) Total cell lysates of SC or *p150^{Glued}* siRNA transfected HeLa cells were analysed by immunoblotting with antibodies to p150^{Glued}, Ninein and Kif3a. Actin served as a loading control. 25 μg of protein lysate was loaded per lane. (**H**) SC and *p150^{Glued}* siRNA transfected HeLa cells were subjected to a microtubule regrowth assay, fixed at the indicated time points and stained with antibodies to α-tubulin to visualize microtubules ('α', green) and γ-tubulin to mark centrosomes ('γ', red). Scale bars indicate 5 μm for all images. For all quantifications at least 100 cells were analysed per experiment ($n = 3$), $P < 0.001$ (paired *t*-test).

established role of Kif3a in IFT, we examined cells that lack Ift88, an IFT protein essential for ciliogenesis (Haycraft *et al*, 2007; Robert *et al*, 2007). In contrast to *Kif3a*$^{-/-}$ MEFs, subdistal appendage organization and centriole cohesion were unaffected in *Ift88* mutants (Supplementary Figure 2). To examine whether Kif3a or Ift88 depend on each other for localization to the mother centriole, we examined the localization of Centrin and either Kif3a or Ift88 in WT, *Kif3a*

mutant cells and *Ift88* mutant cells. The loss of either Kif3a or Ift88 had no effect on the localization of the other protein to centrioles (Supplementary Figure 3), indicating that Kif3a maintains centriole cohesion and organizes subdistal appendages independent of IFT.

p150^{Glued} is also required for centriole cohesion and organization

As Kif3a is critical to localize p150^{Glued} to centrosomes, we investigated whether the loss of p150^{Glued} also alters centriole cohesion and subdistal appendage organization. Depletion of p150^{Glued} by siRNA in HeLa cells and examination of Centrin1 revealed that 69% of cells exhibited premature breakage of centriole cohesion during G1 (Figure 3A–C). This premature loss of centriole cohesion is similar to that caused by displacing Dynactin from centrosomes (Quintyne and Schroer, 2002). Together, these findings reveal that Kif3a recruitment of p150^{Glued} to centrioles is essential for the maintenance of cohesion.

We similarly examined whether loss of p150^{Glued} could account for the subdistal appendage disorganization caused by loss of Kif3a. As in cells lacking Kif3a, p150^{Glued}-depleted centrioles displayed reduced localization of the subdistal appendage proteins Cep170 and Ninein (Figure 3D). The fluorescence intensity of Cep170 and Ninein were decreased by $>75\%$ on p150^{Glued}-depleted centrioles (Figure 3E). These findings are similar to disrupting dynein and dynactin function by overexpressing p150^{Glued}, suggesting that the localization of Cep170 and Ninein is dynactin-dependent (Casenghi *et al*, 2005).

To assess whether the localization of Kif3a to the mother centriole reciprocally depended on p150^{Glued}, we examined the localization of Kif3a after depleting p150^{Glued}. Interestingly, the loss of p150^{Glued} had no effect on the localization of Kif3a to centrosomes (Figure 3F). Thus, Kif3a is required for the localization of p150^{Glued} to the mother centriole, but not vice versa. We confirmed that protein levels of Kif3a and Ninein in p150^{Glued}-depleted cells were unchanged by immunoblot analysis (Figure 3G).

As p150^{Glued} is required for subdistal appendage organization, we assessed whether depletion of p150^{Glued} affected the anchoring of microtubules at the centrosome. We analysed HeLa cells transfected with scrambled or *p150^{Glued}* siRNA for defects in microtubule nucleation (5-min regrowth) or in microtubule anchoring (20-min regrowth). Five minutes following the removal of nocodozale, control cells nucleated a strong aster of microtubules radiating from the centrosome (Figure 3H). In contrast, the centrosomes of p150^{Glued}-depleted cells formed weak asters at the same time point (Figure 3H). Twenty minutes after nocodozale washout, cytoplasmic microtubules had regrown in control and p150^{Glued}-depleted cells. In contrast to control cells, p150^{Glued}-depleted cells had few detectable microtubules anchored at the centrosome (Figure 3H). Together, these findings demonstrate a requirement for p150^{Glued} in organizing of the subdistal appendage and suggesting that the mislocalization of p150^{Glued} and Ninein accounts for the loss of microtubule anchoring at the mother centriole.

p150^{Glued} interacts with the carboxy-terminal region of Kif3a

To understand why Kif3a is required to localize p150^{Glued} to the subdistal appendage and prompted by the ability of *Xenopus* Kinesin II to interact with p150^{Glued} (Deacon *et al*, 2003), we examined whether murine Kif3a and p150^{Glued} interact. Endogenous p150^{Glued} coimmunoprecipitated endogenous Kif3a, revealing that the two proteins interact biochemically (Figure 4A). Reciprocal immunoprecipitation of p150^{Glued} confirmed the specificity of the interaction (Figure 4A).

To gain insight into the functional significance of the Kif3a–p150^{Glued} interaction, we investigated whether the Kif3a motor or cargo-binding domain binds p150^{Glued}. We transfected full-length and truncated versions of Kif3a fused to GFP, immunoprecipitated the exogenous Kif3a using an antibody to GFP, and assessed whether endogenous p150^{Glued} co-precipitated (Figure 4B and C). We detected no interaction between p150^{Glued} and either GFP alone or fused to the amino-terminal motor domain (residues 1–365) of Kif3a. However, the carboxy-terminal cargo-binding 347 amino acids of Kif3a (residues 365–701) were necessary and sufficient for its interaction with p150^{Glued} (Figure 4C).

Given that the motor domain and carboxy-terminal domains of Kif3a were differentially required to interact with p150^{Glued}, we assessed whether the Kif3a deletion mutants could localize to the centriole in *Kif3a$^{-/-}$* MEFs. As expected, the full-length Kif3a fused to GFP localized to the centriole, similar to endogenous Kif3a (Figure 4D). Like full-length Kif3a, the carboxy-terminal half of Kif3a localized to the centriole, whereas GFP and the amino-terminal half of Kif3a did not. Thus, the p150^{Glued} interaction and subdistal appendage localization of Kif3a is dependent upon its carboxy-terminal domain, but not its motor domain.

We assessed whether the Kif3a deletion mutants could restore the localization of p150^{Glued} to the subdistal appendage of mother centrioles in *Kif3a$^{-/-}$* MEFs. The localization of p150^{Glued} to subdistal appendages was not affected by the expression of the truncated forms of Kif3a in WT MEFs (data not shown). *Kif3a$^{-/-}$* MEFs transfected with GFP or the amino-terminal motor domain of Kif3a (residues 1–365) did not restore p150^{Glued} localization to the subdistal appendage. However, expression of the carboxy-terminal domain of Kif3a restored p150^{Glued} localization to the subdistal appendage in *Kif3a* mutant cells as efficiently as full-length Kif3a (Figure 4D and E), suggesting that p150^{Glued} is localized to the subdistal appendage through its interaction with the Kif3a cargo-binding domain and in a manner independent of its motor domain.

To confirm that the motor activity of Kif3a is not required to localize p150^{Glued} to subdistal appendages, we tested the ability of motor dead forms of Kif3a to restore p150^{Glued} localization in *Kif3a* mutant cells (Wiesner *et al*, 2010). Kinesins typically contain an amino-terminal P-loop sequence that binds ATP (Sack *et al*, 1999). Therefore, we expressed motor dead Kif3a containing mutations within its P-loop (lysine 106 and threonine 107 substituted with alanine and asparagine, respectively) in *Kif3a$^{-/-}$* MEFs and assessed p150^{Glued} localization (Wiesner *et al*, 2010). Similar to full-length and the cargo-binding domain, both motor dead forms of Kif3a localized to the centrosome and restored localization of p150^{Glued} to the subdistal appendage (Figure 4F and G). As the motor dead Kif3a could restore p150^{Glued} localization, we assessed whether these mutant constructs could interact with p150^{Glued}. As expected, the

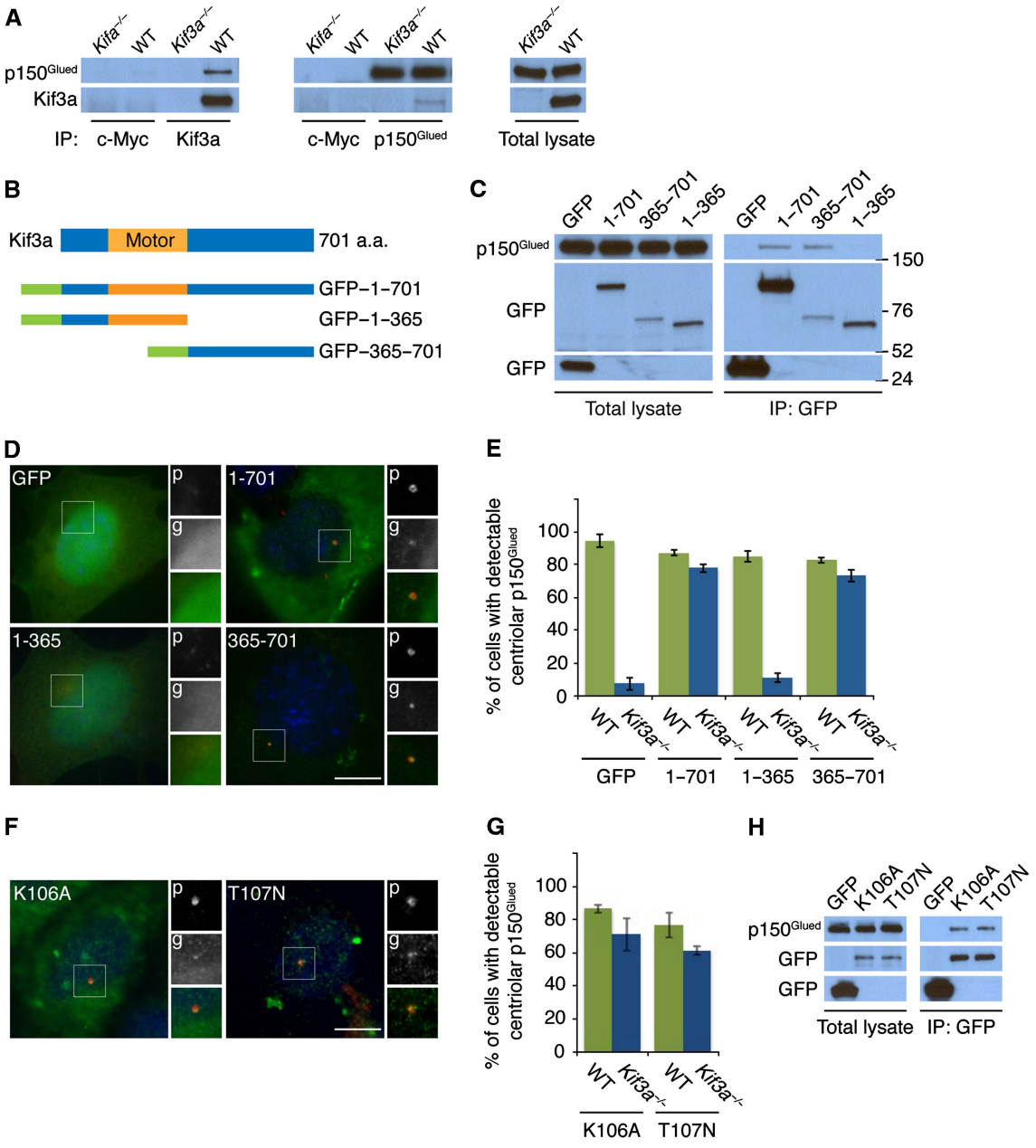

Figure 4 Kif3a is required to localize p150^{Glued} to the subdistal appendage. (**A**) WT and *Kif3a*$^{-/-}$ total cell lysates were subjected to immunoprecipitation of Kif3a, p150^{Glued} and c-Myc, which served as a negative control. Precipitating proteins were subjected to immunoblotting for Kif3a and p150^{Glued}. (**B**) Schematic representations of the motor domain and the truncation mutants of GFP-tagged Kif3a. (**C**) We expressed the indicated GFP-tagged versions of Kif3a in HeLa cells and immunoprecipitated GFP. Endogenous p150^{Glued} and each of the Kif3a fusion proteins were detected by immunoblotting for p150^{Glued} and GFP, respectively. (**D**) Expression of the full-length GFP-tagged Kif3a and the truncated mutant that interacted with p150^{Glued} ('g', green) restored the localization of p150^{Glued} ('p', red) to the subdistal appendage in *Kif3a*$^{-/-}$ cells. (**E**) Quantification of p150^{Glued} localization to the subdistal appendage. (**F**) Expression of the motor dead GFP-tagged Kif3a (K106A and T107N) mutants ('g', green) restored the localization of p150^{Glued} ('p', red) to the subdistal appendage of *Kif3a*$^{-/-}$ MEFs. (**G**) Quantification of p150^{Glued} localization to the subdistal appendage in *Kif3a* mutants. (**H**) We immunoprecipitated the GFP tag of the motor dead Kif3a forms and detected endogenous p150^{Glued} and GFP. At least 100 cells were analysed per experiment ($n=3$), $P<0.001$ (paired *t*-test). Scale bars indicate 5 μm for all images. Source data for this figure is available on the online supplementary information page.

motor dead forms of Kif3a interacted with endogenous p150^{Glued} (Figure 4H). These data indicate that Kif3a localizes to the centrosome and brings p150^{Glued} to the subdistal appendages independent of its motor activity.

Kif3a is required for microtubule organization and anchoring

The Dynactin component p150^{Glued} is required for microtubule anchoring at the mother centriole (Quintyne and Schroer, 2002). As Kif3a is required for the localization of p150^{Glued} to the subdistal appendage, we examined whether the anchoring of centrosomal microtubules also depends upon Kif3a. We analysed the microtubule cytoskeleton and PCM of WT and *Kif3a*$^{-/-}$ MEFs by examining the organization of α-tubulin and γ-tubulin. WT cells displayed radially arranged microtubules, the majority of which originated at the centrosome (Figure 5A, left panel). In contrast, the microtubules of *Kif3a* mutant cells did not

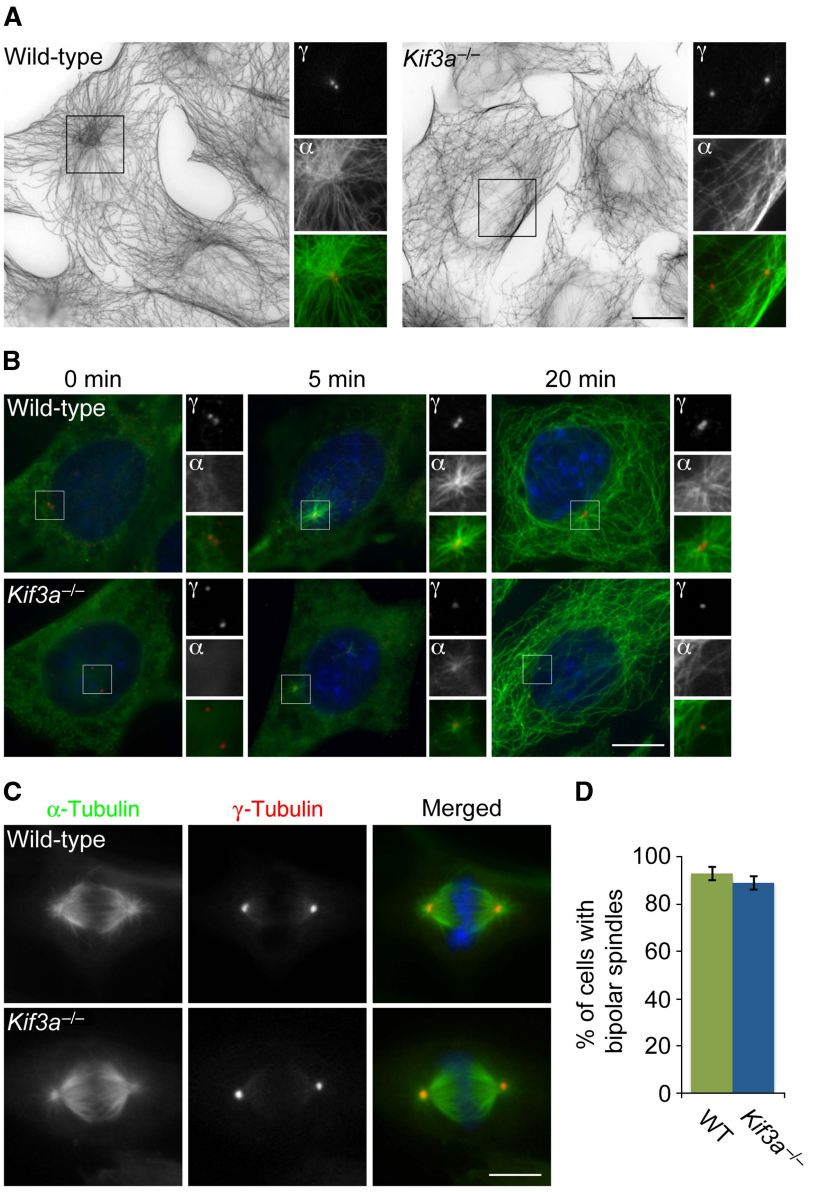

Figure 5 Kif3a is essential for microtubule anchoring at the mother centriole. (**A**) Immunofluorescence analysis of WT or *Kif3a*$^{-/-}$ MEFs co-stained for α-tubulin ('α', green) and γ-tubulin ('γ', red). Large figures are inverted images of α-tubulin staining. The inset shows magnified images of the boxed region. (**B**) WT and *Kif3a*$^{-/-}$ MEFs were subjected to a microtubule regrowth assay, fixed at the indicated time points and stained with antibodies to α-tubulin to visualize microtubules ('α', green) and γ-tubulin to mark centrosomes ('γ', red). (**C**) Mitotic WT and *Kif3a*$^{-/-}$ MEFs were stained for α-tubulin and γ-tubulin to visualize mitotic spindles and poles, respectively. (**D**) Percentage of WT and *Kif3a*$^{-/-}$ cells with bipolar mitotic spindles. At least 100 cells were analysed per experiment ($n = 3$). Scale bars indicate 5 μm for images in a, 3 μm for images in (**B**).

originate from the centrosome and were chaotically oriented (Figure 5A, right panel).

In another test of microtubule anchoring, we assessed whether *Kif3a* mutant cells could anchor microtubules at the mother centriole following microtubule depolymerization. Five minutes following removal of nocodazole, WT cells radiated a strong microtubule aster from the centrosome (Figure 5B). In contrast, *Kif3a* mutant cells only supported weak asters at the same time point. Twenty minutes after nocodazole removal, microtubules had similarly regrown in WT and *Kif3a*$^{-/-}$ cells. However, in contrast to the centrosomally anchored microtubules observed in WT cells, the microtubules of *Kif3a* mutant cells were not anchored at centrosomes (Figure 5B). The defect in microtubule organization is similar to that caused by p150^{Glued} depletion, suggesting that Kif3a localization of p150^{Glued} and Ninein to the subdistal appendages supports microtubule assembly and anchoring at the centrosome.

Because previous studies suggested that Kinesin II function was required for chromosomal stability and bipolar spindle formation (Haraguchi *et al*, 2006), we examined whether *Kif3a*$^{-/-}$ MEFs undergo abnormal mitoses. Visualization of spindle microtubules and poles revealed that WT and *Kif3a* mutants both form bipolar spindles that properly align chromosomes at the metaphase plate (Figure 5C). Quantification indicated that there was no change in the number of abnormal spindles in WT and *Kif3a*$^{-/-}$ cells (Figure 5D).

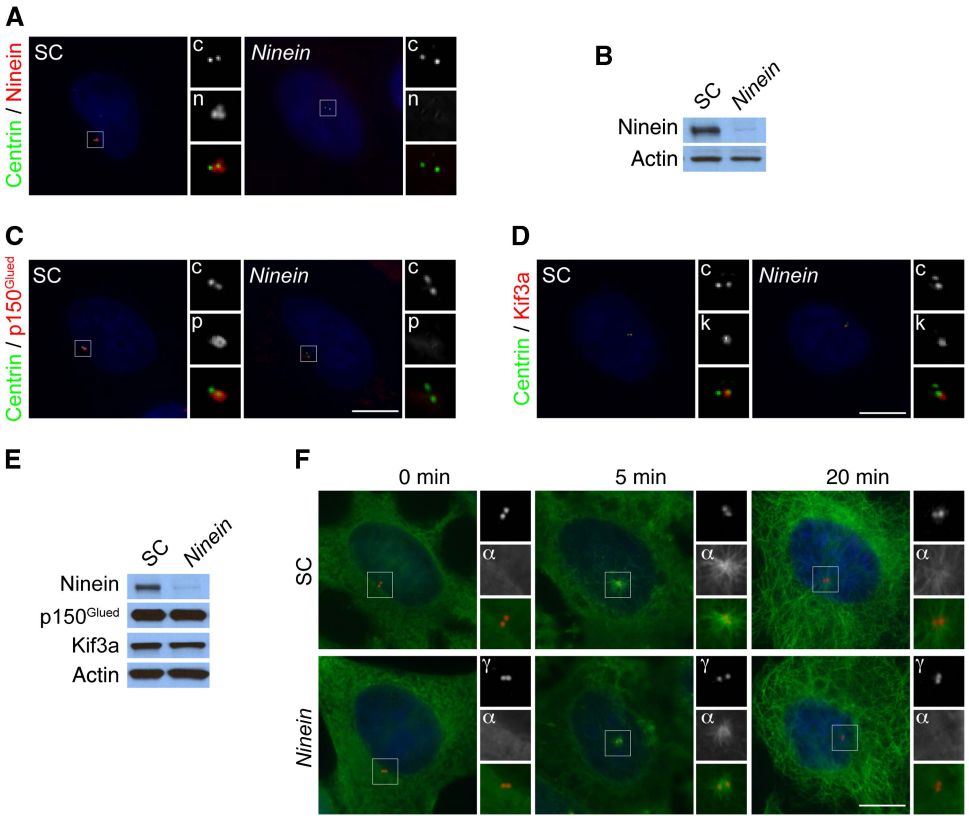

Figure 6 Ninein is required for subdistal appendage organization and microtubule anchoring. (**A**) Immunofluorescence microscopy analysis of SC or *Ninein* siRNA transfected HeLa cells co-stained for Ninein ('n', red) and Centrin ('c', green) to visualize centrioles. (**B**) Total cell lysates of scramble control (SC) or *Ninein* siRNA transfected HeLa cells were analysed by immunoblotting for Ninein. Actin served as a loading control. 25 μg of protein lysate was loaded per lane. (**C**) The depletion of Ninein disrupted the localization of the subdistal appendage protein $p150^{Glued}$ ('p', red). Cells were stained for Centrin ('c', green) to visualize centrioles in G1. (**D**) Immunofluorescence images of SC and *Ninein* siRNA-treated HeLa cells co-stained for Centrin ('c', green) and Kif3a ('k', red). (**E**) Total cell lysates of SC or *Ninein*-depleted cells were analysed by immunoblotting with antibodies to Ninein, $p150^{Glued}$ and Kif3a. Actin served as a loading control. 25 μg of protein lysate was loaded per lane. (**F**) SC and *Ninein* siRNA transfected HeLa cells were subjected to a microtubule regrowth assay, fixed at the indicated time points and stained with antibodies to α-tubulin to visualize microtubules ('α', green) and γ-tubulin to mark centrosomes ('γ', red). Scale bars indicate 5 μm for all images.

Ninein is required for centriole organization and microtubule anchoring

As Kif3a and $p150^{Glued}$ are required for the localization of Ninein to the subdistal appendage and for centriole cohesion, we examined whether centriole attachment depends upon Ninein. Depletion of *Ninein* by siRNA in HeLa cells and examination of centrioles revealed that centriole cohesion remained intact (Figure 6A and B), indicating that Kif3a and $p150^{Glued}$ maintain centriole cohesion independent of Ninein.

To assess whether the localization of $p150^{Glued}$ and Kif3a to the mother centriole reciprocally depend on Ninein, we examined the localization of these proteins after depleting Ninein. Interestingly, $p150^{Glued}$ was absent from centrosomes in Ninein-depleted cells, suggesting that Ninein and $p150^{Glued}$ require each other to localize to the subdistal appendage (Figure 6C). In contrast, the centrosome localization of Kif3a was unaltered in Ninein-depleted cells (Figure 6D). We confirmed that protein levels of Kif3a and $p150^{Glued}$ in Ninein-depleted cells were unchanged by immunoblot analysis (Figure 6E). Thus, Kif3a is required for the localization of $p150^{Glued}$ and Ninein to the mother centriole, but not vice versa.

Given the mislocalization of Ninein in *Kif3a* mutants and $p150^{Glued}$-depleted cells, we examined whether the siRNA depletion of *Ninein* was sufficient to evoke a loss of microtubule anchoring at the centrosome. We assessed whether microtubule anchoring is abrogated in Ninein-depleted cells by performing a microtubule regrowth assay. Similar to the loss of Kif3a and $p150^{Glued}$, Ninein-depleted cells nucleated weak microtubule asters 5 min after nocodazole removal and failed to anchor microtubules at the centrosome after 20 min (Figure 6F). Taken together, our data indicate that Kif3a recruits $p150^{Glued}$ to the centrosome. In turn, $p150^{Glued}$ recruits Ninein to the subdistal appendage to facilitate microtubule anchoring at the mother centriole.

Kif3a is required for the formation of ciliary basal feet

The relationship of subdistal appendages to basal feet is unclear, but they form at similar positions along the proximal–distal length of the centriole and are comprised of some of the same proteins, suggesting that they have similar etiologies (Anderson, 1972). We examined centrosomes in over 50 serum deprived WT, $Kif3a^{-/-}$ and $Ift88^{-/-}$ MEFs by serial, ultrathin section electron microscopy. WT cells formed primary cilia with associated basal bodies bearing one or two basal feet (Figure 7A, top panel). Although basal bodies docked at the plasma membrane in $Kif3a^{-/-}$ cells, these basal bodies lacked both primary cilia and basal feet

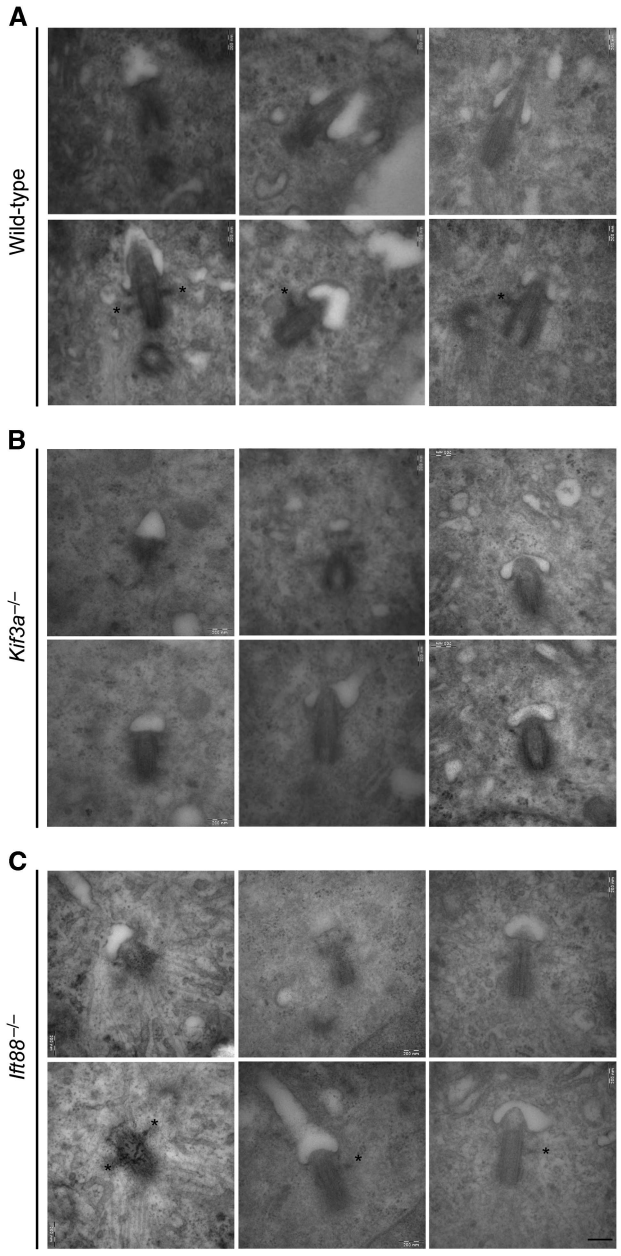

Figure 7 Kif3a is required for ciliary basal foot formation. Serial ultrathin sections electron micrographs of basal bodies in (**A**) WT, (**B**) *Kif3a*$^{-/-}$ and (**C**) *Ift88*$^{-/-}$ MEFs. Two consecutive sections reveal the presence of a primary cilium in three WT cells. Primary cilia are absent in *Kif3a* and *Ift88* mutant MEFs. Ciliary basal feet (asterisks) are detected in the subdistal region of basal bodies in WT and *Ift88*$^{-/-}$ MEFs, but are not found in *Kif3a*$^{-/-}$ MEFs. Basal feet in at least 10 serially sectioned samples were analysed per experiment ($n = 3$). Scale bars indicate 200 nm for all images.

(Figure 7B, middle panel). Like *Kif3a*$^{-/-}$ cells, *Ift88*$^{-/-}$ cells lack primary cilia and basal bodies dock to the plasma membrane, but unlike *Kif3a*$^{-/-}$ cells, *Ift88*$^{-/-}$ cells have basal bodies with intact subdistal appendages (Pazour *et al*, 2000; Supplementary Figure 2A). Interestingly, basal bodies in *Ift88*$^{-/-}$ cells also form basal feet (Figure 7C, bottom panel). These findings indicate that, as with centriole cohesion and subdistal appendage formation, Kif3a has an indispensable role in basal foot formation that is independent of IFT and ciliogenesis.

Discussion

We have found that Kif3a is a component of the mother centriole that regulates the organization and function of the subdistal appendage. Kif3a interacts with p150^{Glued} through its carboxy-terminal cargo-binding domain to bring p150^{Glued} to the subdistal appendages of the mother centriole. As loss of Kif3a or depletion of p150^{Glued} both inhibit the localization of Ninein and Cep170 to subdistal appendages, it is likely that Kif3a recruits p150^{Glued} to the mother centriole, which in turn recruits other subdistal appendage components such as Ninein and Cep170.

However, Kif3a and p150^{Glued} do not extensively colocalize at the mother centriole. Kif3a localizes to a single focus at the same proximal–distal position along the mother centriole as subdistal appendages, whereas p150^{Glued} forms a ring consistent with localization to the subdistal appendages themselves. These observations raise the possibility that the interaction of Kif3a with p150^{Glued} is transient, with Kif3a bringing p150^{Glued} to the centriole, but not anchoring p150^{Glued} at the subdistal appendages. Given that the localization of Kif3a to the centrosome precedes both p150^{Glued} and Ninein, Kif3a may provide a centrosomal docking site on the mother centriole for the subdistal appendage to reform upon exit from mitosis.

Like Kif3a, the mother centriolar protein ODF2 localizes to a single focus on mother centrioles and is required to recruit Ninein to the subdistal appendage (Nakagawa *et al*, 2001; Kunimoto *et al*, 2012). Given that the localization of Kif3a and ODF2 is distinct from that of the subdistal appendage proteins that depend on them, it remains unclear how Kif3a and ODF2 coordinate the recruitment of subdistal appendage components. One possibility is that Dynactin must bind to both Dynein and Kinesin II to move to the minus ends of microtubules where unloading of subdistal appendage components onto the centrioles occurs.

Kif3a is also required for centriole cohesion during G1, similar to the Dynactin component, p150^{Glued} (Quintyne *et al*, 1999; Quintyne and Schroer, 2002). The cargo-binding domain of Kif3a interacts with p150^{Glued} to localize it to the subdistal appendages. Curiously, the depletion of Ninein leads to the mislocalization of p150^{Glued}, but does not lead to the loss of centriole cohesion. One possibility is that a Kif3a–p150^{Glued} complex functions outside of the centrosome to recruit factors that maintain centriole cohesion. It will be interesting to investigate how Kif3a and p150^{Glued} complex interact with other proteins involved in centriole attachment.

We found that Kif3a, p150^{Glued} and Ninein are required for microtubule anchoring. Furthermore, we found that Kif3a localization does not require Ninein, suggesting that the microtubule anchoring defect in Kif3a mutants is due to the mislocalization of Ninein.

Complex cellular events, including basal body organization and the assembly of functional IFT particles, must be orchestrated to support ciliogenesis (Marshall and Rosenbaum, 2001; Song and Dentler, 2001; Graser *et al*, 2007; Vladar and Stearns, 2007). We found that subdistal appendage and basal foot formation require Kif3a, but not Ift88, indicating that the ciliogenic function of Kinesin II is not limited to IFT, but that Kif3a also participates in centriole organization. The genetic requirement for Kif3a in the formation of both subdistal appendages and basal feet may underscore many other commonalities between them, including composition and

origin (Seeley and Nachury, 2010; Kunimoto *et al*, 2012). Future experiments to determine the components of the basal foot and their relationship to Kif3a and the subdistal appendage may uncover the molecular mechanism underlying basal foot formation. In summary, we demonstrate that Kif3a is an essential component of the mother centriole ensuring the integrity of the subdistal appendage and that the loss of Kif3a abrogates microtubule anchoring and ciliary basal foot formation.

Materials and methods

Antibodies

Antibodies used in this study are the following: anti-Cep170 (Invitrogen and gift of G Guarguaglini, Sapienza, University of Rome, Italy), anti-Ninein (Millipore, Bethyl and gift of S Tsukita, Osaka University, Japan), anti-Centrin1 (Proteintech), anti-Centrin 20H5 (Millipore and gift of J Salisbury, Mayo Clinic), anti-Centrin3 (gift of M Bornens, Centre National de la Recherche Scientifique–Pierre Fabre, France), anti-polyglutamylated tubulin (gift of C Janke, Centre de Recherche de Biochimie Macromoléculaire, France), anti-p150^{Glued} (BD Biosciences, Santa Cruz Biotechnology and gift of E Holzbaur, University of Pennsylvania), anti-Kif3a (Sigma, Proteintech, BD Biosciences and Covance), anti-Centrobin (Abcam), anti-α-tubulin and γ-tubulin (Sigma), anti-Ift88 and CP110 (Proteintech), anti-GFP (Abcam, Santa Cruz Biotechnologies and Invitrogen). Alexa-conjugated secondary antibodies, Hoechst 33342 and DAPI were obtained from Molecular Probes (Invitrogen).

Cell culture, plasmid and siRNA transfections

Kif3a$^{-/-}$ and *Ift88*$^{-/-}$ MEFs were derived from embryonic days 8.5 and 10.5 littermate embryos, respectively, along with MEFs from littermate WT controls. MEFs were grown in DMEM (UCSF tissue culture facility) supplemented with 15% FBS (Invitrogen), Glutamax-I (Invitrogen), sodium pyruvate, non-essential amino acids, penicillin and streptomycin. MEFs were subsequently immortalized with SV40 large T antigen. MEFs conditional for *Kif3a* were cultured as described previously (Corbit *et al*, 2008). HeLa cells (UCSF tissue culture facility) were cultured in Advanced DMEM (Invitrogen) supplemented with 2% FBS and Glutamax-I. For transfection of HeLa cells and MEFs, Fugene6 (Roche) or Lipofectamine PLUS (Invitrogen) transfection reagents were used according to the manufacturer's instructions. The following siRNA sequences were used: Scramble control (SC): 5′-AAUUCUCCGAACG UGUCACGUdtdt-3′ (Qiagen), human *p150^{Glued}*: 5′-GCCUUGAACAG UUCCAUCAdtdt-3′ (Delgehyr *et al*, 2005) human Stealth *Ninein #1*: 5′-GCCAGGGUUAGUAAUGUCUUCUUGU-3′ (Invitrogen) and human Stealth *Ninein #2*: 5′-GGAGGCGGAGCUCUCUGAAGUUA AA-3′ (Invitrogen). HeLa cells were transfected with siRNA using Oligofectamine (Invitrogen) and analysed 48 h later.

Immunofluorescence

To visualize centrosome proteins in MEFs, cells were fixed in −20 °C methanol for 3 min. To detect Kif3a in MEFs, cells were pre-extracted for 30 s in PEM-P buffer (100 mM Pipes, 10 mM EGTA, 1 mM MgCl and 0.1% Triton-X-100) followed by fixation in 4% paraformaldehyde in PBS for 8 min and then postfixed in methanol for 30 s. Following fixation, cells were incubated in blocking solution (0.1% Triton-X-100, 0.01% NaN_3 and 2.5% BSA in PBS) overnight at 4 °C. Primary and secondary antibodies were diluted in blocking solution and incubated with cells at room temperature for 1 h. Coverslips were mounted using Gelvatol mounting media and imaged with an inverted Axio Observer D1 (Zeiss) or a Deltavision deconvolution microscope (Applied Precision), image processing and measurements were completed with Fiji image processing software and Adobe Photoshop.

Immunoprecipitation and immunoblotting

Cells were harvested using a cell scraper and lysed on ice for 10 min in lysis buffer (50 mM Tris–HCl pH7.4, 150 mM NaCl, 1% NP-40) supplemented with a protease inhibitor cocktail (Calbiochem). Lysates were clarified (13 000 r.p.m., 4 °C, 10 min) and the protein concentrations were determined using the Bradford assay (Bio-Rad). For each immunoprecipitation reaction, 500 μg of total lysate was incubated with 2 μg of antibody for 2 h and then incubated with protein G-Agarose (Invitrogen) for an additional hour at 4 °C. Immunocomplexes were washed three times in lysis buffer and subsequently boiled in 2 × Laemmli reducing buffer. Samples were separated by SDS–PAGE, transferred onto nitrocellulose (Whattman) and then subjected to immunoblot analysis using ECL Lightening Plus (Perkin-Elmer).

Transmission electron microscopy

Cells were plated on two-well Permanox slides (Nunc), fixed in 3.5% glutaraldehyde in 0.1 M phosphate buffer (PB) for 1 h at room temperature, then washed three times in 0.1 M PB. Cells were postfixed in 2% osmium tetroxide for 2 h, dehydrated and embedded in Durcupan (Fluka). Serial ultrathin sections (70 nm) were cut with a diamond knife to reconstruct whole cilia, stained with lead citrate and examined using a FEI Tecnai Spirit electron microscope.

Supplementary data

Supplementary data are available at *The EMBO Journal* Online (http://www.embojournal.org).

Acknowledgements

This work was funded by grants from NIH (T32HL007731) to AK, the NIH (R01AR054396, R01GM095941), the Burroughs Wellcome Fund, the Packard Foundation, and the Sandler Family Supporting Foundation to JFR.

Author contributions: AK and JFR designed the experiments. AK and AS derived wild-type, *Kif3a*$^{-/-}$, and *Ift88*$^{-/-}$ mouse embryonic fibroblasts. JFR cloned the Kif3a fusion constructs. ATK, MSSP, and JMGV prepared and imaged the electron microscopy samples. AK and JFR interpreted the data and wrote the paper.

Conflict of interest

The authors declare that they have no conflict of interest.

References

Anderson RG (1972) The three-dimensional structure of the basal body from the rhesus monkey oviduct. *J Cell Biol* **54:** 246–265

Bobinnec Y, Khodjakov A, Mir LM, Rieder CL, Edde B, Bornens M (1998) Centriole disassembly *in vivo* and its effect on centrosome structure and function in vertebrate cells. *J Cell Biol* **143:** 1575–1589

Boisvieux-Ulrich E, Sandoz D (1991) Determination of ciliary polarity precedes differentiation in the epithelial cells of quail oviduct. *Biol Cell* **72:** 3–14

Bornens M (2002) Centrosome composition and microtubule anchoring mechanisms. *Curr Opin Cell Biol* **14:** 25–34

Casenghi M, Barr FA, Nigg EA (2005) Phosphorylation of Nlp by Plk1 negatively regulates its dynein-dynactin-dependent targeting to the centrosome. *J Cell Sci* **118:** 5101–5108

Chang P, Giddings Jr. TH, Winey M, Stearns T (2003) Epsilon-tubulin is required for centriole duplication and microtubule organization. *Nat Cell Biol* **5:** 71–76

Corbit KC, Shyer AE, Dowdle WE, Gaulden J, Singla V, Chen MH, Chuang PT, Reiter JF (2008) Kif3a constrains beta-catenin-dependent Wnt signalling through dual ciliary and non-ciliary mechanisms. *Nat Cell Biol* **10:** 70–76

Deacon SW, Serpinskaya AS, Vaughan PS, Lopez Fanarraga M, Vernos I, Vaughan KT, Gelfand VI (2003) Dynactin is required for bidirectional organelle transport. *J Cell Biol* **160:** 297–301

Delgehyr N, Sillibourne J, Bornens M (2005) Microtubule nucleation and anchoring at the centrosome are independent processes linked by ninein function. *J Cell Sci* **118:** 1565–1575

Finetti F, Paccani SR, Riparbelli MG, Giacomello E, Perinetti G, Pazour GJ, Rosenbaum JL, Baldari CT (2009) Intraflagellar transport is required for polarized recycling of the TCR/CD3 complex to the immune synapse. *Nat Cell Biol* **11:** 1332–1339

Graser S, Stierhof YD, Lavoie SB, Gassner OS, Lamla S, Le Clech M, Nigg EA (2007) Cep164, a novel centriole appendage protein required for primary cilium formation. *J Cell Biol* **179:** 321–330

Guarguaglini G, Duncan PI, Stierhof YD, Holmstrom T, Duensing S, Nigg EA (2005) The forkhead-associated domain protein Cep170 interacts with Polo-like kinase 1 and serves as a marker for mature centrioles. *Mol Biol Cell* **16:** 1095–1107

Haraguchi K, Hayashi T, Jimbo T, Yamamoto T, Akiyama T (2006) Role of the kinesin-2 family protein, KIF3, during mitosis. *J Biol Chem* **281:** 4094–4099

Haycraft CJ, Zhang Q, Song B, Jackson WS, Detloff PJ, Serra R, Yoder BK (2007) Intraflagellar transport is essential for endochondral bone formation. *Development* **134:** 307–316

Holley MC, Afzelius BA (1986) Alignment of cilia in immotile-cilia syndrome. *Tissue Cell* **18:** 521–529

Ishikawa H, Kubo A, Tsukita S (2005) Odf2-deficient mother centrioles lack distal/subdistal appendages and the ability to generate primary cilia. *Nat Cell Biol* **7:** 517–524

Ishikawa H, Marshall WF (2011) Ciliogenesis: building the cell's antenna. *Nat Rev Mol Cell Biol* **12:** 222–234

Kunimoto K, Yamazaki Y, Nishida T, Shinohara K, Ishikawa H, Hasegawa T, Okanoue T, Hamada H, Noda T, Tamura A, Tsukita S (2012) Coordinated ciliary beating requires Odf2-mediated polarization of basal bodies via basal feet. *Cell* **148:** 189–200

Louie RK, Bahmanyar S, Siemers KA, Votin V, Chang P, Stearns T, Nelson WJ, Barth AI (2004) Adenomatous polyposis coli and EB1 localize in close proximity of the mother centriole and EB1 is a functional component of centrosomes. *J Cell Sci* **117:** 1117–1128

Marshall WF, Rosenbaum JL (2001) Intraflagellar transport balances continuous turnover of outer doublet microtubules: implications for flagellar length control. *J Cell Biol* **155:** 405–414

Marszalek JR, Ruiz-Lozano P, Roberts E, Chien KR, Goldstein LS (1999) Situs inversus and embryonic ciliary morphogenesis defects in mouse mutants lacking the KIF3A subunit of kinesin-II. *Proc Natl Acad Sci USA* **96:** 5043–5048

Mirzadeh Z, Han YG, Soriano-Navarro M, Garcia-Verdugo JM, Alvarez-Buylla A (2010) Cilia organize ependymal planar polarity. *J Neurosci* **30:** 2600–2610

Mitchell B, Jacobs R, Li J, Chien S, Kintner C (2007) A positive feedback mechanism governs the polarity and motion of motile cilia. *Nature* **447:** 97–101

Mitchell B, Stubbs JL, Huisman F, Taborek P, Yu C, Kintner C (2009) The PCP pathway instructs the planar orientation of ciliated cells in the Xenopus larval skin. *Curr Biol* **19:** 924–929

Mogensen MM, Malik A, Piel M, Bouckson-Castaing V, Bornens M (2000) Microtubule minus-end anchorage at centrosomal and non-centrosomal sites: the role of ninein. *J Cell Sci* **113**(Pt 17): 3013–3023

Moritz M, Braunfeld MB, Guenebaut V, Heuser J, Agard DA (2000) Structure of the gamma-tubulin ring complex: a template for microtubule nucleation. *Nat Cell Biol* **2:** 365–370

Nakagawa Y, Yamane Y, Okanoue T, Tsukita S (2001) Outer dense fiber 2 is a widespread centrosome scaffold component preferentially associated with mother centrioles: its identification from isolated centrosomes. *Mol Biol Cell* **12:** 1687–1697

Nonaka S, Tanaka Y, Okada Y, Takeda S, Harada A, Kanai Y, Kido M, Hirokawa N (1998) Randomization of left-right asymmetry due to loss of nodal cilia generating leftward flow of extraembryonic fluid in mice lacking KIF3B motor protein. *Cell* **95:** 829–837

Ou YY, Mack GJ, Zhang M, Rattner JB (2002) CEP110 and ninein are located in a specific domain of the centrosome associated with centrosome maturation. *J Cell Sci* **115:** 1825–1835

Paintrand M, Moudjou M, Delacroix H, Bornens M (1992) Centrosome organization and centriole architecture: their sensitivity to divalent cations. *J Struct Biol* **108:** 107–128

Pazour GJ, Dickert BL, Vucica Y, Seeley ES, Rosenbaum JL, Witman GB, Cole DG (2000) Chlamydomonas IFT88 and its mouse homologue, polycystic kidney disease gene tg737, are required for assembly of cilia and flagella. *J Cell Biol* **151:** 709–718

Pedersen LB, Geimer S, Rosenbaum JL (2006) Dissecting the molecular mechanisms of intraflagellar transport in chlamydomonas. *Curr Biol* **16:** 450–459

Piel M, Meyer P, Khodjakov A, Rieder CL, Bornens M (2000) The respective contributions of the mother and daughter centrioles to centrosome activity and behavior in vertebrate cells. *J Cell Biol* **149:** 317–330

Quintyne NJ, Gill SR, Eckley DM, Crego CL, Compton DA, Schroer TA (1999) Dynactin is required for microtubule anchoring at centrosomes. *J Cell Biol* **147:** 321–334

Quintyne NJ, Schroer TA (2002) Distinct cell cycle-dependent roles for dynactin and dynein at centrosomes. *J Cell Biol* **159:** 245–254

Rayner CF, Rutman A, Dewar A, Greenstone MA, Cole PJ, Wilson R (1996) Ciliary disorientation alone as a cause of primary ciliary dyskinesia syndrome. *Am J Respir Crit Care Med* **153:** 1123–1129

Robert A, Margall-Ducos G, Guidotti JE, Bregerie O, Celati C, Brechot C, Desdouets C (2007) The intraflagellar transport component IFT88/polaris is a centrosomal protein regulating G1-S transition in non-ciliated cells. *J Cell Sci* **120:** 628–637

Rosenbaum JL, Witman GB (2002) Intraflagellar transport. *Nat Rev Mol Cell Biol* **3:** 813–825

Sack S, Kull FJ, Mandelkow E (1999) Motor proteins of the kinesin family. Structures, variations, and nucleotide binding sites. *Eur J Biochem* **262:** 1–11

Seeley ES, Nachury MV (2010) The perennial organelle: assembly and disassembly of the primary cilium. *J Cell Sci* **123:** 511–518

Sfakianos J, Togawa A, Maday S, Hull M, Pypaert M, Cantley L, Toomre D, Mellman I (2007) Par3 functions in the biogenesis of the primary cilium in polarized epithelial cells. *J Cell Biol* **179:** 1133–1140

Song L, Dentler WL (2001) Flagellar protein dynamics in Chlamydomonas. *J Biol Chem* **276:** 29754–29763

Takahashi M, Yamagiwa A, Nishimura T, Mukai H, Ono Y (2002) Centrosomal proteins CG-NAP and kendrin provide microtubule nucleation sites by anchoring gamma-tubulin ring complex. *Mol Biol Cell* **13:** 3235–3245

Takeda S, Yonekawa Y, Tanaka Y, Okada Y, Nonaka S, Hirokawa N (1999) Left-right asymmetry and kinesin superfamily protein KIF3A: new insights in determination of laterality and mesoderm induction by kif3A-/- mice analysis. *J Cell Biol* **145:** 825–836

Vladar EK, Stearns T (2007) Molecular characterization of centriole assembly in ciliated epithelial cells. *J Cell Biol* **178:** 31–42

Wiesner C, Faix J, Himmel M, Bentzien F, Linder S (2010) KIF5B and KIF3A/KIF3B kinesins drive MT1-MMP surface exposure, CD44 shedding, and extracellular matrix degradation in primary macrophages. *Blood* **116:** 1559–1569

Wong C, Stearns T (2003) Centrosome number is controlled by a centrosome-intrinsic block to reduplication. *Nat Cell Biol* **5:** 539–544